









# Modeling and Simulation of an Orthodontic System of a Real Patient Starting from CBCT Images

Dragos-Laurentiu Popa<sup>1</sup>(✉) , Ionela Teodora Dascalu<sup>2</sup>, Daniela Tarnita<sup>1</sup> ,  
Alina Duta<sup>1</sup> , Gabriel Buciu<sup>3</sup>, Ludmila Sass<sup>1</sup> , Daniela Vintila<sup>1</sup> ,  
and Stelian-Mihai-Sever Petrescu<sup>2</sup> 

<sup>1</sup> Faculty of Mechanics, University of Craiova, 200512 Craiova, Romania  
dragos.popa@edu.ucv.ro

<sup>2</sup> Faculty of Dentistry, University of Medicine and Pharmacy of Craiova, 200349 Craiova, Romania

<sup>3</sup> Faculty of Health Care, Titu Maiorescu University, 210102 Targu Jiu, Romania

**Abstract.** The paper first presented the stages of obtaining a virtual model of a female patient, aged 13 years and who had multiple dental malpositions. The patient underwent a CT scan, and CT images were initially processed using the InVesalius program and three-dimensional geometries were obtained, both for the mandible and jaw, but also for the dental structure. These primary geometries were processed, edited and transformed using Reverse Engineering techniques in the Geomagic program. Dental alveoli were obtained in SolidWorks using CAD methods and techniques. Bracket elements and orthodontic wires were also generated in SolidWorks. Interference solids have been removed by various processes so that the model is geometrically accurate. Finally, these structures formed of virtual solids recomposed the orthodontic system of the analyzed patient. The custom model was exported to Ansys, where it was analyzed and result maps were obtained. Finally, interesting conclusions and some clinical observations were highlighted.

**Keywords:** Computer Aided Design · Orthodontic System · Finite Elements Method

## 1 Introduction

Malocclusions represent imbalances in the processes of formation and growth of the stomatognathic system. They have a growing prevalence from one generation to the next as a result of climate change, soil, air and water pollution, with unfavorable consequences for the nutritional pattern. Thus, diet along with other etiopathogenic factors contribute to increasingly complex changes in the somatic development of the whole body and, implicitly, of the cephalic extremity.

The standards of dento-facial aesthetics have been a standard in the evaluation of the harmony of the human body since antiquity. The first attempts to correct malocclusions

were mentioned 3000 years ago. However, they were first scientifically approached in the late 19th century.

The association of new medical imaging techniques in orthodontic practice has led to further studies on craniofacial development. These investigations include optical coherence tomography (OCT) and computed tomography (CBCT) [1–11].

Also, the transformation of these CBCT images into three-dimensional geometry, leaves room for various analyzes, used in engineering, such as determining the mechanical behavior by using techniques specific to the finite element method (FEM).

## 2 The Three-Dimensional Model of a Patient’s Orthodontic System

A 14-year-old female patient was analyzed. To obtain the patient’s dental geometry, CBCT images made before the first orthodontic wires were used. The InVesalius program was used, which, based on the shades of gray in the images, creates three-dimensional geometric structures by choosing different tissue filter from the program’s database [12–18]. Thus, by choosing from the program menu, Bone type filter, the primary geometry for such structures can be obtained as can be seen in Fig. 1.

Also, by modifying the Bone filter in Enamel, the primary geometry of the teeth of the studied patient was obtained. Figure 2 shows this primary model.

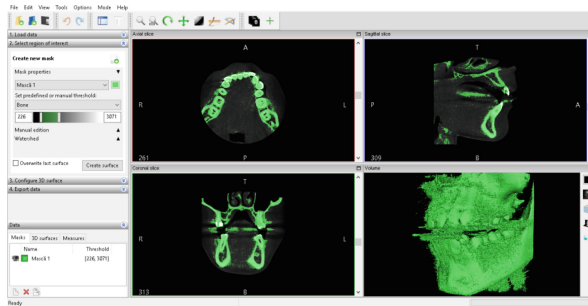


**Fig. 1.** CBCT images of the patient studied uploaded to InVesalius.

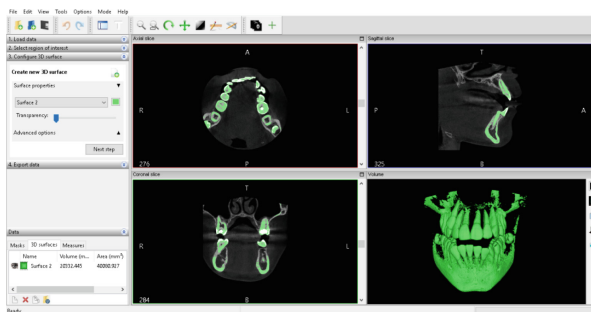


**Fig. 2.** CBCT images of the patient studied using the Enamel filter.

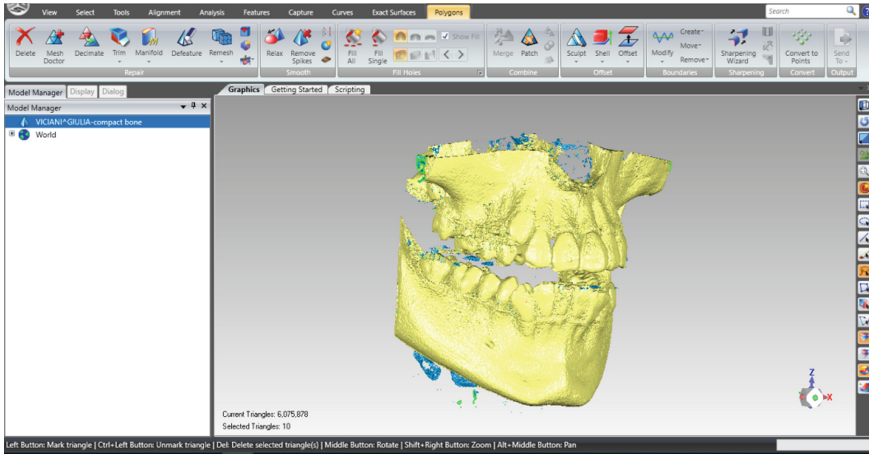


**Fig. 3.** Model imported into Geomagic software.

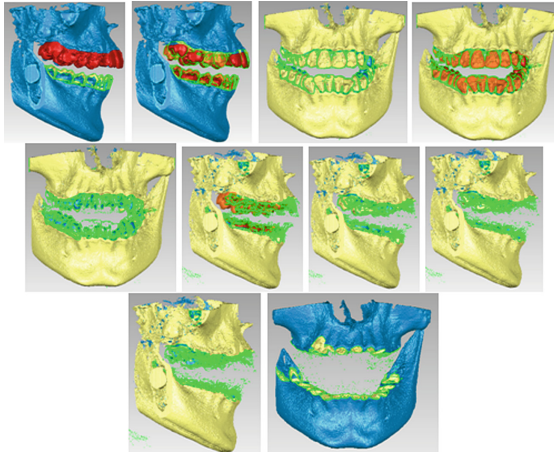


**Fig. 4.** Stages of removal operations.

The model obtained in InVesalius was exported to Geomagic for processing and editing. The Geomagic program is mainly used for processing 3D scans or files containing so-called “point clouds”, using Reverse Engineering techniques [3–7]. This model, in the primary phase, is shown in Fig. 3.

In the Geomagic program, that “point cloud” was transformed into elementary triangular surfaces. Initially, the model had 6,075,878 triangular surfaces. It was intended, in a first stage, to remove from this model the surfaces that define the teeth in order to obtain only the bone structures [7]. These surfaces were successively selected and removed. Stages of removal operations are shown in Fig. 4.

After this first stage of processing the model had 3,281,334 elementary triangular surfaces. Because, in order to obtain a completely closed surface, different “filling”

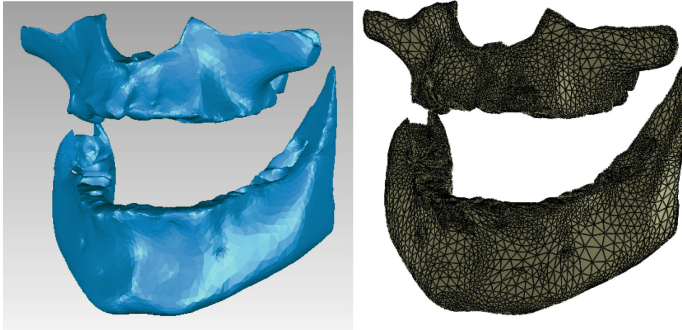


**Fig. 5.** The final model of bone components in Geomagic and SolidWorks.

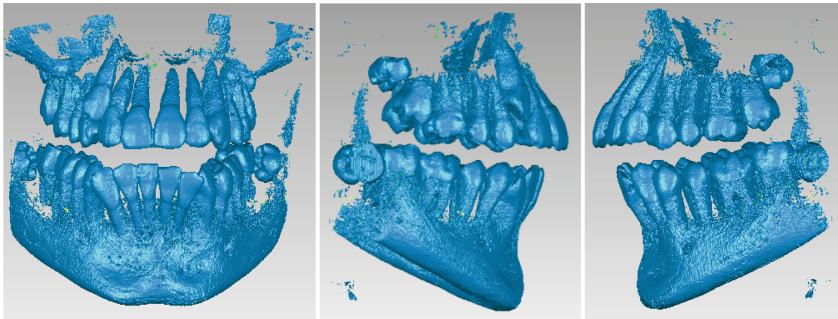


**Fig. 6.** The initial model imported into Geomagic.

operations were used. To eliminate some self-intersections surface, very sharp edges, but also other irregularities, the Mesh Doctor command was applied. Subsequently, several commands for decimating the number of elementary, finishing, correcting triangular surfaces were applied. The number of triangular areas was first reduced from 3,217,246 to 1,427,112 and finally to 86,165. Figure 5 shows the final model of the bone components in Geomagic, then in SolidWorks, where it was automatically transformed into a virtual solid.

Next, starting from the initial geometry obtained in InVesalius using the Enamel filter, this, in the form of a “point cloud” was imported into Geomagic for reverse engineering specific processing, with the aim of obtaining virtual solids for the dental structure. Figure 6 shows this model which was automatically transformed into triangular surfaces, initially numbering 3,426,848.

The model was processed using bone component geometry removal operations, decimation operations, non-conforming surface removal operations, decimation operations, etc. After applying these operations, the model had 1,695,551 elementary surfaces. An important problem that appear during the application of various operations in Geomagic was that of interference between the models of different teeth, a situation that does not correspond to reality. In order to eliminate these deficiencies of the model, the interfering

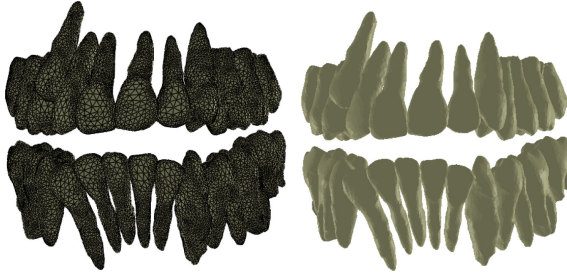


**Fig. 7.** The dental model in SolidWorks using two viewing modes.

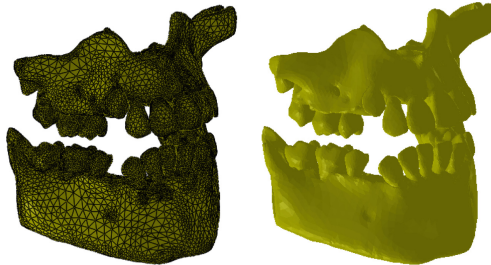


**Fig. 8.** The complete dental structure of the studied patient (two ways of visualization).

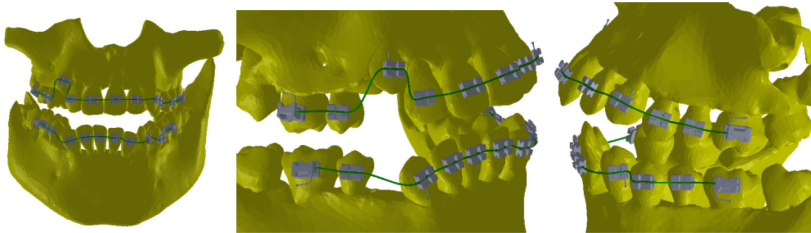


**Fig. 9.** The final model of the orthodontic system of the studied patient.

surfaces were manually removed and replaced with others that do not have this disadvantage. Finally, other reverse engineering operations were applied to the model. The final model of the dental structure, which had 156,042 elementary triangular surfaces. Finally, the model was imported into SolidWorks where it was automatically transformed into independent virtual solids, as shown in Fig. 7.

In order to obtain the complete model of the dental structure of the studied patient, the two models (bone fragments and teeth) were loaded in the Assembly module of SolidWorks. Given that these models have a common global coordinate system because they come from the same set of CBCT images, the main planes defining the coordinate system were aligned and the model shown in Fig. 8 was obtained.

To avoid interference between the virtual solids, the volumes of the teeth were extracted from the bone components using CAD commands and techniques, these cavities representing the dental alveoli. Known CAD methods and techniques were used to obtain the models of the bracket elements. Previously, the box with the bracket elements was scanned 2D, and it was scaled so that the image is on a natural scale and, thus, a series of measurement scan be made on this image. The electronic caliper was also used to measure different sizes. Using the data obtained through measurements and using CAD techniques and methods, all the bracket elements were modeled. Using similar CAD techniques, the final models of the other bracket elements were obtained.

In a first stage, these bracket elements were placed on the tooth surfaces. Also, three points have been defined on each bracket that will be used to define the Path curve of the orthodontic wires. In real world, these elements are fixed with a special adhesive. The Sweep shape was used to model the orthodontic wire, defining the Path curve in the context of the ensemble. This curve is defined by the three points located on each bracket element. After defining the Path curves for the two orthodontic wires, knowing the diameter of the wire (0.3556 mm, ie 0.014 inches), the two models were generated in the context of the assembly. The final model of the personalized orthodontic system is shown in Fig. 9.

### 3 Analysis of the Mechanical Behavior of the Personalized Orthodontic System

Next, the virtual model of the custom system was imported into Ansys Workbench. Orthodontic wires were initially present in the model, as well as bracket elements. The Engineering Data module of the Ansys Workbench program defined the material characteristics of the components of the analyzed system, as shown in Table 1. We consider that the all materials have orthotropic properties.

Next, the model was divided into tetrahedral finite elements, using the default characteristics. Figure 10 shows the finite element structure of the analyzed system.

Next, the elements considered fixed, namely the jaw and the mandible, were indicated. Then, the forces with a value of 1 N were determined for each bracket-type element, as shown in Fig. 11, most researchers claim that the optimal force exerted during an orthodontic treatment should be up to 1 N. Also, the bracket elements were removed from the simulation in order not to create elastic reactions [8–11].

**Table 1.** Physical properties of materials used in simulation.

Component	Material	Density	Young's Modulus	Poisson's Ratio
Bracket	Ni + Cr Alloy	8500 kg/m <sup>3</sup>	$2.1 \cdot 10^{11}$ Pa	0.31
Maxillary, mandible	Bone	1400 kg/m <sup>3</sup>	$1 \cdot 10^{10}$ Pa	0.31
Teeth	Enamel	2958 kg/m <sup>3</sup>	$7.79 \cdot 10^{10}$ Pa	0.3
Orthodontic wires	Ni + Ti Alloy	6450	$8.3 \cdot 10^{10}$ Pa	0.33

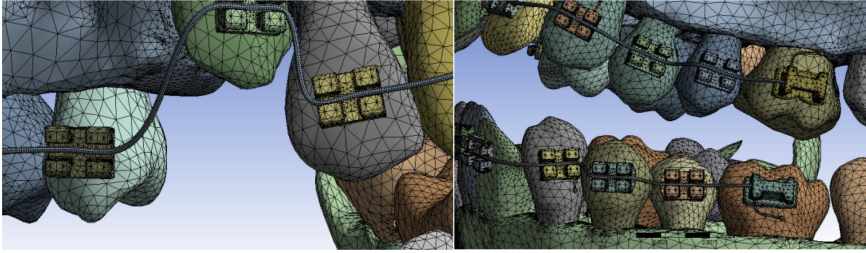


Fig. 10. The finite element structure of the analyzed system (a spatial view and two details).

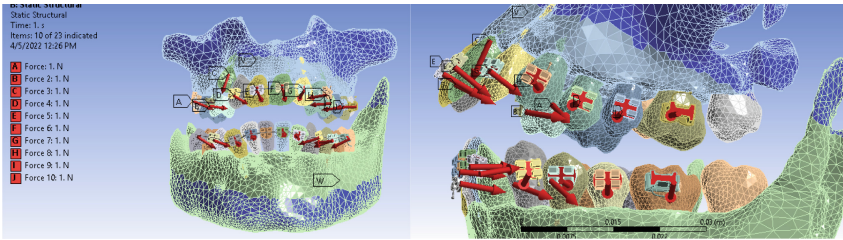


Fig. 11. The forces defined in Ansys for the personalized model analyzed (a view and a detail).

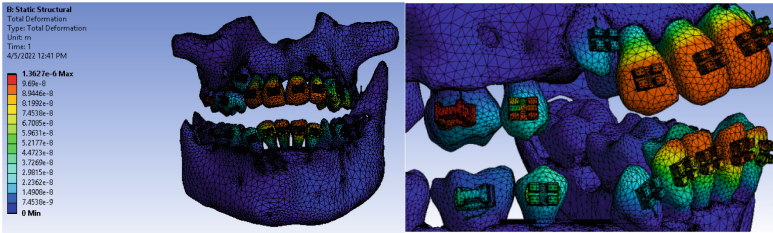


Fig. 12. Displacement maps.

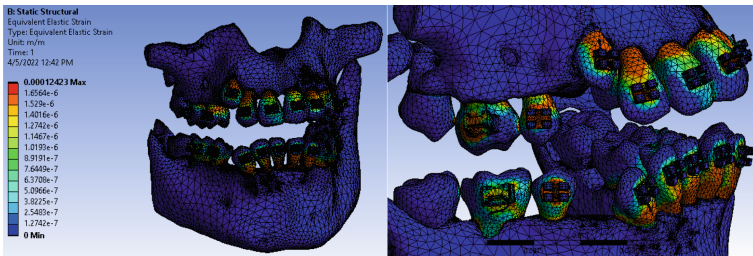


Fig. 13. Strain maps.

After running the application, maps of displacements (Fig. 12), strains (Fig. 13), stresses (Fig. 14) and deformation energies (Fig. 15) were obtained, similar simulations in [12–21].

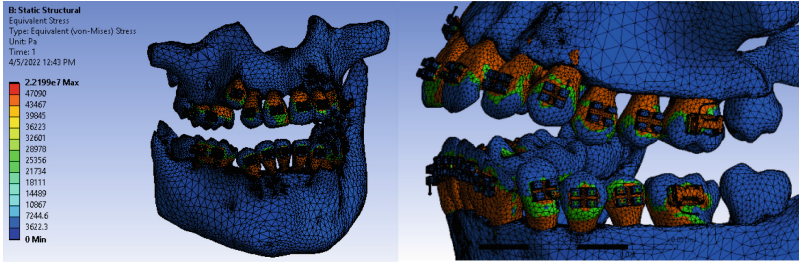


Fig. 14. Stress maps.

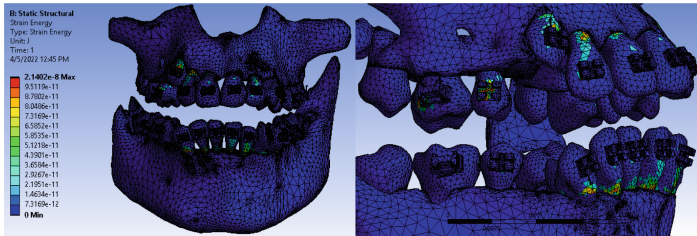


Fig. 15. Strain energy maps.

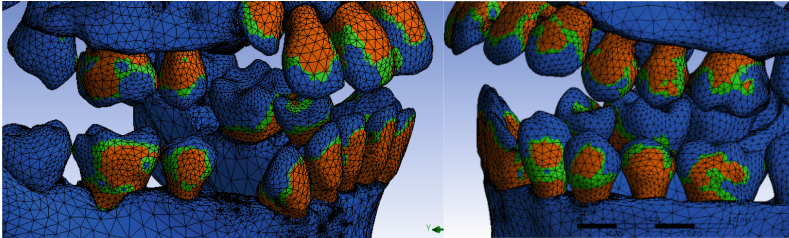


Fig. 16. Maximum stress detected under bracket elements (bracket elements have been visually removed).

## 4 Conclusions

The paper presents the main steps for obtaining a virtual orthodontic system, based on CT images of a patient undergoing several stages of treatment. This paper, practically, demonstrates that any orthodontic system can be recomposed in virtual space and, personalized situations can be created and analyzed. By analyzing the simulation results, which consist of maps of displacements, strains, stresses and strain energies, the following conclusions can be drawn:

- The maximum displacements were  $1.3627 \cdot e^{-7}$  m, and the maximum values were found on the anterior faces of the teeth, but also on the bracket type elements;
- The maximum strains were 0.00012423 mm/mm, and the highest values were in the area of the dental roots, but also on the bracket type elements;



- The maximum stresses were  $2,2199 \cdot e^7$  Pa, these being located in the areas of the dental roots and on the bracket type elements;
- The maximum strain energies had the value of  $21402 \cdot e^{-8}$  J and were found on the dental roots.

At all these maximum values are within acceptable limits. Based on these conclusions, a series of clinical observations can be explained. By the action of orthodontic wires, the bone cells in the mandible and jaw disappear in the direction of the action of forces, but appear on the opposite side of the tooth, so that the teeth are mechanically stable. It is also observed that most of the values determined by simulation are maximum on the dental roots, which explains certain very rare situations, when certain teeth can be severely damaged. It has been determined by specific OCT techniques that, although the beneficial effect of orthodontic techniques based on orthodontic wires is recognized, under the bracket elements, the stress are increased, and, in reality, under them, the appearance of cracks was observed (Fig. 16).

Simulation evaluation for 1N forces is only a quantitative analysis, but in the future our team will develop another algorithm that will allow the exact calculation of each force for each bracket element.

## References

1. Petrescu, S.M.S., Țuculină, M.J., Georgescu, D., Mărășescu, F.I., Manolea, H.O., Țircă, T., Popescu, M., Nicola, A., Voinea-Georgescu, R., Dascălu, I.T.: Epidemiological study of malocclusions in schoolchildren between 6 and 14 years old from Gorj County, Romania. *Romanian Journal of Oral Rehabilitation* 13(3), 92–102 (2021).
2. Petrescu, S.M.S., Țuculină, M.J., Osiac, E., Camen, A., Sălan, A.I., Mărășescu, F.I., Nicola, A.G., Bechir, E.S., Dascălu, I.T.: Use of optical coherence tomography in orthodontics. *Experimental and therapeutic medicine* 22(1424), 1–7 (2021).
3. Popa, D.L., Buciu, G., Calin, D.C., Popkonstantinović, B., Poenaru, F.: CAD, CAE and rapid prototyping methods applied in long bones orthopaedics. *FME Transactions* 47(2), 279–286 (2019).
4. Popa, D.L., Poenaru, F., Gherghina, G., Tutunea, D., Popkonstantinovic, B.: New CAD Techniques Used for Virtual Bone Models Applied in Orthopedics. *Journal of Industrial Design and Engineering Graphics* 12(1), 133–136 (2017).
5. Vatu, M., Vintilă, D., Popa, D.L., Mercuț, R., Popescu, S.M., Vintila, G.: Simulations Using Finite Element Method Made on a Personalized Dental System. *Advanced Engineering Forum* 34, 175–182 (2019).
6. Vatu, M., Vintilă, D., Popa, D.L., Mercuț, R., Popescu, S.M., Vintila, G.: Determining Mechanical Causes that Produce Dental Wear Using Finite Element Method. *Applied Mechanics and Materials* 896, 15–22 (2020).
7. Popa, D.L., Duță, A., Tutunea, D., Gherghina, G., Buciu, G., Calin, D.C.: Virtual Methods Applied to Human Bones and Joints Re-Construction Used for Orthopedic Systems. *Applied Mechanics and Materials* 822, 160–165 (2016).
8. Theodorou, C.I., Kuijpers-Jagtman, A.M., Bronkhorst, E.M., Wagener, F.A.: Optimal force magnitude for bodily orthodontic tooth movement with fixed appliances: A systematic review. *Am. J. Orthod. Dentofac. Orthop.* 156, 582–92 (2019).

9. Cuoghi, O.A., Topolski, F., de Faria, L.P., Ervolino, E., Micheletti, K.R., Miranda-Zamalloa, Y.M., Moresca, R., Moro, A., de Mendonça, M.R.: Correlation between pain and hyalinization during tooth movement induced by different types of force. *Angle Orthod.* 89, 788–96 (2019).
10. Romanyk, D.L., Vafaeian, B., Addison, O., Adeeb, S.: The use of finite element analysis in dentistry and orthodontics: Critical points for model development and interpreting results. *Semin. Orthod.* 26, 162–73 (2020).
11. Luchian, I., Mărțu, M.A., Tatarciuc, M., Scutariu, M.M., Ioanid, N., Păsărin, L., Kappenberg-Nițescu, D.C., Sioustis, I.A., Solomon, S.M.: Using FEM to Assess the Effect of Orthodontic Forces on Affected Periodontium. *Appl Sci.* 11, 7183 (2021).
12. Tarnita, D., Tarnita, D.N., Bizdoaca, N., Popa, D., Tarnita, C.E., Cismaru, F.: Modular orthopedic devices based on shape memory alloys. *SYROM 2009*, 709–721 (2010).
13. Tarnita, D., Tarnita, D.N., Popa, D., Grecu, D., Tarnita, R.: The Method of Finite Element applied to the study of stress distribution of tibia. *Biomaterials and Biomechanics: Fundamentals and Clinical Applications*, Essen, Germany (2005).
14. Vatu, M., Vintila, D., Mercut, R., Popescu, S.M., Popa, D.L., Petrovici, I.L., Vintila, G., Pitru, A.: Three-dimensional modeling of the dental-maxillary system. *Journal of Industrial Design and Engineering Graphics* 14(1), 207–210 (2019).
15. Tarnita, D., Boborelu, C., Popa, D., Tarnita, D.N.: Design and Finite Element Analysis of a New Spherical Prosthesis-Elbow Joint Assembly. *New Advances in Mechanism and Machine Science*, 127–135 (2018).
16. Calin, D., Tarniță, D., Popa, D., Calafeteanu, D., Tarnita, D.N.: Virtual model and simulation of the normal and affected human hip joint. *Applied Mechanics and Materials* 823, 167–172 (2016).
17. Calin, D.C., Popa, D.L., Grecu, A.F.: Virtual Experimental Analyzes of the Normal and Arthrotic Hip. *Applied Mechanics and Materials* 896, 3–14 (2020).
18. Tarnita, D., Popa, D., Tarnita, D.N., Bizdoaca, N.G.: Considerations on the dynamic simulation of the 3D model of the human knee joint. *BIO Materialien Interdisciplinary/Journal of Functional Materials, Biomechanics and Tissue Engineering* 231, (2006).
19. Petrovici, I.L., Tenovici, M.C., Vaduva, R.C., Tarnita, D.N., Vintila, G., Popa, D.L.: About Three-Dimensional Models of Osteosynthesis Systems. *Journal of Industrial Design and Engineering Graphics* 14(1), 159–162 (2019).
20. Tarnita, D., Popa, D., Boborelu, C., Dumitru, N., Calafeteanu, D., Tarnita, D.N.: Experimental bench used to test human elbow endoprosthesis. *New Trends in Mechanism and Machine Science*, 669–677 (2015).
21. Ciunel, S., Popa, D.L., Dumitru, N.: Studies about Movement Biofidelity of a Dummy Neck Used in an Impact Testing Device. *Applied Mechanics and Materials* 371, 539–543 (2013).

**Open Access** This chapter is licensed under the terms of the Creative Commons Attribution-NonCommercial 4.0 International License (<http://creativecommons.org/licenses/by-nc/4.0/>), which permits any noncommercial use, sharing, adaptation, distribution and reproduction in any medium or format, as long as you give appropriate credit to the original author(s) and the source, provide a link to the Creative Commons license and indicate if changes were made.

The images or other third party material in this chapter are included in the chapter's Creative Commons license, unless indicated otherwise in a credit line to the material. If material is not included in the chapter's Creative Commons license and your intended use is not permitted by statutory regulation or exceeds the permitted use, you will need to obtain permission directly from the copyright holder.

